International Journal of Heat and Mass Transfer 51 (2008) 5154–5159

Contents lists available at ScienceDirect

International Journal of Heat and Mass Transfer

journal homepage: www.elsevier.com/locate/ijhmt

Forced convection of non-Newtonian fluids on a heated flat plate

Lun-Shin Yao [a,*], Md. Mamun Molla [b]

[a] Department of Mechanical and Aerospace Engineering, Arizona State University, AZ 876108, USA
[b] Department of Mechanical Engineering, University of Glasgow, Glasgow G12 8QQ, UK

ARTICLE INFO

Article history:
Received 19 October 2007
Received in revised form 3 April 2008
Available online 23 July 2008

ABSTRACT

Forced convective heat transfer due to a non-Newtonian fluid flowing past a flat plate has been investigated using a modified power-law viscosity model. This model does not contain physically unrealistic limits; consequently, no irremovable singularities are introduced into boundary-layer formulations for such fluids. Therefore, the boundary-layer equations can be solved by (numerically) marching downstream from the leading edge as is common for boundary layers involving Newtonian fluids. For shear-thinning and shear-thickening fluids, non-Newtonian effects are illustrated via velocity and temperature distributions, shear stresses, and heat transfer rates. The most significant effects occur near the leading edge, gradually tailing off far downstream where the variation of shear stresses becomes smaller.

1. Introduction

The interest in heat transfer problems involving power-law, non-Newtonian fluids has grown in the past half century. Recently, an excellent sequence of lectures on non-Newtonian fluids was given by Hinch [1]. It appears that Acrivos [2], a frequently cited paper, was the first to consider boundary-layer flows for such fluids. Since then, a large numbers of relevant papers have been published due to their importance in chemicals, foods, polymers, molten plastics, petroleum production, and other natural phenomena. A complete survey of this literature is impractical; however, a few items are listed here to provide starting points for a broader literature search [2–15].

Two widespread mistakes appear continuously in papers studying boundary layers of power-law, non-Newtonian fluids. The first is that few authors recognize that a length scale is introduced by the use of power-law correlations; consequently, boundary-layer problems with power-law, non-Newtonian fluids cannot have simple self-similar solutions. Nevertheless, it is a common practice to ignore, without justification, the dependence of boundary-layer solutions on the streamwise coordinate. It has been demonstrated in [14,15] that such a self-similar solution is only valid at the leading edge of the boundary layer. This similarity solution is a natural upstream condition, which is needed to integrate the boundary-layer equations in the streamwise direction from the leading edge. The mathematical structure of the boundary layer is similar to that of the mixed-convection boundary layer on a vertical heated plate [16].

The second concern is related to the unrealistic physical results, introduced by the traditional power-law correlation, that viscosity either vanishes or becomes infinite in the limits of large or small shear rates, respectively. This usually occurs at the leading edge of a flat plate, or along the outer edge of the boundary layer where it matches with the outer inviscid flow. Thus, traditional power-law correlations introduce non-removable singularities into boundary-layer formulations leading to infinite or zero viscosity. Without recognizing the cause of such unrealistic conditions, complex multi-layer structures have sometimes been introduced to overcome mathematical difficulties in order to obtain solutions of a non-physical formulation [12,13], or a "false" starting process has been used to integrate boundary-layer equations slightly downstream from the leading edge to avoid the leading-edge region.

The new modified power-law correlation is sketched in Fig. 2 for various values of the power index n. It is clear that the new correlation does not contain the two physically unrealistic limits associated with traditional power-law correlations, and fits better with the measured viscosity data [1]. The constants in the proposed model are fixed with available measurements and are described in detail in [14]. The boundary-layer formulation on a flat plate is described and numerically solved in [14], and the associated heat transfer for two different heating conditions is reported in [15]. An oil was selected in the study of [14,15]; its power-law index of 0.95 is only slightly different from the Newtonian value, $n = 1$. In this paper, the analysis is extended to fluids whose power-law indexes are 0.6, 0.8, 1, 1.2, and 1.4 in order to fully demonstrate the impact of the new correlation.

It is worthy to note that the variation of viscosity for shear-thickening cases can lead to rather large viscosities at a leading edge; in turn, this can cause the Reynolds number to be so small as to invalidate the boundary-layer approximation. Thus, applying the analysis reported in this paper requires judgment. A brief discussion is provided about the flow structure near the leading edge

* Corresponding author. Tel.: +1 480 965 5914.
E-mail address: ls_vao@asu.edu (L.-S. Yao).

0017-9310/$ - see front matter © 2008 Elsevier Ltd. All rights reserved.
doi:10.1016/j.ijheatmasstransfer.2008.04.010

Nomenclature

C	constant
C_f	Shear stress
D	non-dimensional viscosity of the fluid
K	thermal conductivity
l	reference length scale of the plate
n	non-Newtonian power-law index
Nu	Nusselt number
Re	Reynolds number
$(\bar{u},\bar{v})$	fluid velocities in the $(\bar{x},\bar{y})$ directions, respectively
(U,V)	dimensionless fluid velocities in the (ξ,η) directions, respectively
U_0	free stream velocity
T	dimensional temperature of the fluid
T_w	surface temperature
T_∞	ambient temperature

Greek symbols

ξ	axial direction along the plate
η	pseudo-similarity variable
γ	shear rate
ρ	fluid density
ν	viscosity of the non-Newtonian fluid
ν_1	reference viscosity of the fluid
α	thermal diffusivity
θ	dimensionless fluid temperature

of a sharp flat plate and the nature of the associated singularity in order to elucidate the physics of flow and its removability in Section 3.

2. Formulation of problem

A steady laminar boundary layer of a non-Newtonian fluid along a semi-infinite heated flat plate has been studied. The viscosity depends on the dominant fluid shear rate and is correlated by a modified power-law. We consider shear-thinning and shear-thickening situations of non-Newtonian fluids. It is assumed that the surface temperature of the plate is T_w, where $T_w > T_\infty$. Here T_∞ is the ambient temperature of the fluid and T is the temperature of the fluid. The coordinate system is shown in Fig. 1.

The equations governing the flow and heat transfer are

$$\frac{\partial \bar{u}}{\partial \bar{x}} + \frac{\partial \bar{v}}{\partial \bar{y}} = 0, \tag{1}$$

$$\bar{u}\frac{\partial \bar{u}}{\partial \bar{x}} + \bar{v}\frac{\partial \bar{u}}{\partial \bar{y}} = \frac{\partial}{\partial \bar{y}}\left(\nu \frac{\partial \bar{u}}{\partial \bar{y}}\right), \tag{2}$$

$$\bar{u}\frac{\partial T}{\partial \bar{x}} + \bar{v}\frac{\partial T}{\partial \bar{y}} = \alpha \frac{\partial^2 T}{\partial \bar{y}^2}, \tag{3}$$

where $(\bar{u},\bar{v})$ are velocity components along the $(\bar{x},\bar{y})$ axes, T is the temperature, and α is the thermal diffusivity of the fluid. The viscosity is correlated by a modified power-law, which is

$$\nu = \frac{K}{\rho}\left|\frac{\partial \bar{u}}{\partial \bar{y}}\right|^{n-1} \quad \text{for } \bar{\gamma}_1 \leqslant \left|\frac{\partial \bar{u}}{\partial \bar{y}}\right| \leqslant \bar{\gamma}_2. \tag{4}$$

The constants $\bar{\gamma}_1$ and $\bar{\gamma}_2$ are two threshold shear rates, ρ is the density of the fluid and K is a dimensional constant, whose dimension depends on the power-law index n. The values of these constants can be determined by matching with measurements. Outside of the above range, viscosity is assumed constant; its value can be fixed with data given in Fig. 2.

The boundary conditions for the present problem are

$$\begin{aligned} &\bar{u} = \bar{v} = 0, \quad T = T_w \text{ at } \bar{y} = 0, \\ &\bar{u} \to U_0, \quad T \to T_\infty \text{ as } \bar{y} \to \infty. \end{aligned} \tag{5}$$

We now introduce the following non-dimensional variables and transform boundary-layer equations to parabolic coordinates (ξ,η):

$$\begin{aligned} &\xi = x = \frac{\bar{x}}{l}, \quad \eta = \bar{y}\left(\frac{U_0}{2\bar{x}\nu_1}\right)^{1/2}, \quad U = \frac{\bar{u}}{U_0}, \quad V = \bar{v}\left(\frac{2\bar{x}}{U_0\nu_1}\right)^{1/2}, \\ &\theta = \frac{T - T_\infty}{T_w - T_\infty}, \quad Re = \frac{U_0 l}{\nu_1}, \quad D = \frac{\nu}{\nu_1}, \end{aligned} \tag{6}$$

where ν_1 is the reference viscosity, θ is the dimensionless temperature of the fluid, Re is the Reynolds number. The length scale associated with the non-Newtonian power-law [14] is

$$l = C^{\frac{2}{1-n}}\left[\left(\frac{K}{\rho}\right)^2 \frac{1}{\nu_1^{n+1}}\right]^{\frac{1}{n-1}} U_0^3. \tag{7}$$

Substituting variables (6) into Eqs. (1)–(4) leads to the following equations

$$(2\xi)\frac{\partial U}{\partial \xi} - \eta\frac{\partial U}{\partial \eta} + \frac{\partial V}{\partial \eta} = 0, \tag{8}$$

$$(2\xi)U\frac{\partial U}{\partial \xi} + (V - \eta U)\frac{\partial U}{\partial \eta} = \frac{\partial}{\partial \eta}\left[D\frac{\partial U}{\partial \eta}\right], \tag{9}$$

$$(2\xi)U\frac{\partial \theta}{\partial \xi} + (V - \eta U)\frac{\partial \theta}{\partial \eta} = \frac{1}{Pr}\frac{\partial^2 \theta}{\partial \eta^2}, \tag{10}$$

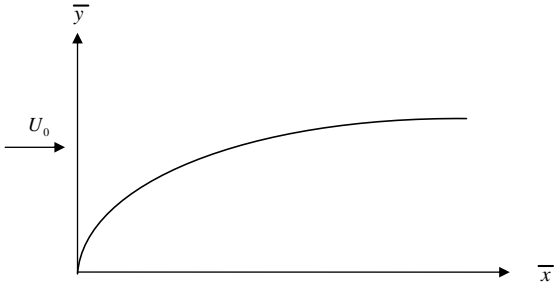

Fig. 1. Coordinates.

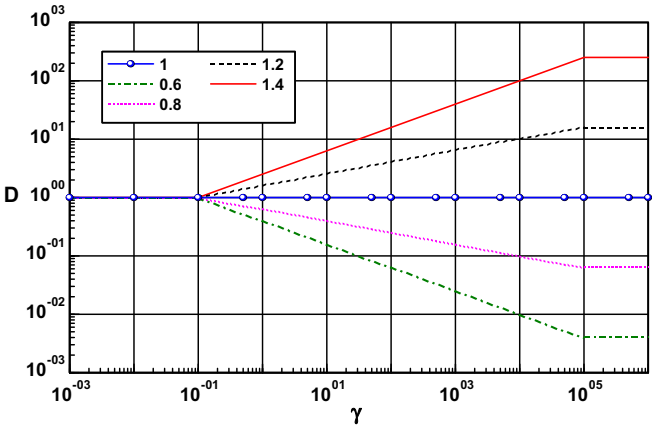

Fig. 2. Modified power-law correlation.

where Pr is the Prandtl number,

$$D=\begin{cases}1, & \gamma\leqslant\gamma_1\\ \left|\frac{\gamma}{\gamma_1}\right|^{n-1}, & \gamma_1\leqslant|\gamma|\leqslant\gamma_2,\quad \text{and } \gamma=(2\xi)^{-1/2}\frac{\partial U}{\partial\eta}.\\ \left|\frac{\gamma_2}{\gamma_1}\right|^{n-1}, & \gamma\geqslant\gamma_2\end{cases}\tag{11}$$

The boundary conditions (5) become

$$\begin{aligned}&U=V=0,\quad \theta=1 \text{ at } \eta=0,\\ &U\to 1,\quad \theta\to 0 \text{ as } \eta\to\infty.\end{aligned}\tag{12}$$

Eqs. (8)–(10) can be solved by marching downstream with the upstream condition satisfying the following ordinary differential equations by taking the limit of (8)–(10) as $\xi\to 0$. The result is

$$-\eta\frac{\partial U}{\partial\eta}+\frac{\partial V}{\partial\eta}=0,\tag{13}$$

$$(V-\eta U)\frac{\partial U}{\partial\eta}=\frac{\partial}{\partial\eta}\left[D\frac{\partial U}{\partial\eta}\right],\tag{14}$$

$$(V-\eta U)\frac{\partial\theta}{\partial\eta}=\frac{1}{Pr}\frac{\partial^2\theta}{\partial\eta^2},\tag{15}$$

The solution of the above equation is the Blasius solution for a fluid with constant viscosity D.

Eqs. (8)–(10) and (13)–(15) are discretized by a central-difference scheme for the diffusion term and a backward-difference a scheme for the convection terms; finally we get a system of implicit tri-diagonal algebraic system of equations. The algebraic equations have been solved by a double-sweep technique. In the computation the continuity equation is directly solved for the normal velocity V. Hence, the truncation errors are $O(\Delta\xi)$. The computation is started from $\xi=0$, and then marches downstream to $\xi=100$. After several test runs, convergent results are obtained by using $\Delta\xi=2\times10^{-9}$ and $\Delta\eta=0.001$ near the leading edge, say $\xi=0.0$–10^{-5}; afterwards $\Delta\xi$ is gradually increased to $\Delta\xi=0.01$.

In practical applications, the physical quantities of primary interest are the skin-friction coefficient C_f and the Nusselt number Nu, respectively; they are defined by

$$C_f(2\xi)^{1/2}=\left[D\frac{\partial U}{\partial\eta}\right]_{\eta=0},\tag{16}$$

$$Nu(2\xi)^{-1/2}=-\left(\frac{\partial\theta}{\partial\eta}\right)_{\eta=0}.\tag{17}$$

3. Results and discussion

Numerical results are presented for the non-Newtonian power-law fluids of shear-thinning ($n=0.6$, 0.8) and shear-thickening ($n=1.2$, 1.4) cases along with those for a Newtonian fluid ($n=1.0$). The velocity and temperature distribution appear in Figs. 3–5; the skin-friction coefficient and the Nusselt number appear in Figs. 6–8 for large Prandtl number. The singularity experienced at the leading edge for the traditional power-law correlation has been successfully removed by using the modified power-law correlation. Since the shear tress at the leading edge is inversely proportional to $\sqrt{2\xi}$, and so is infinite there, $D=(\gamma_2/\gamma_1)^{n-1}$ at the leading edge.

Fig. 3a–d show the velocity distribution as a function of η at selected ξ locations for various values of the power-law index n. From Fig. 3a, it is seen that for the shear-thinning fluids ($n<1$), the velocity speeds up rapidly due the reduction of viscosities near the leading edge. Since the local Reynolds number is larger for a

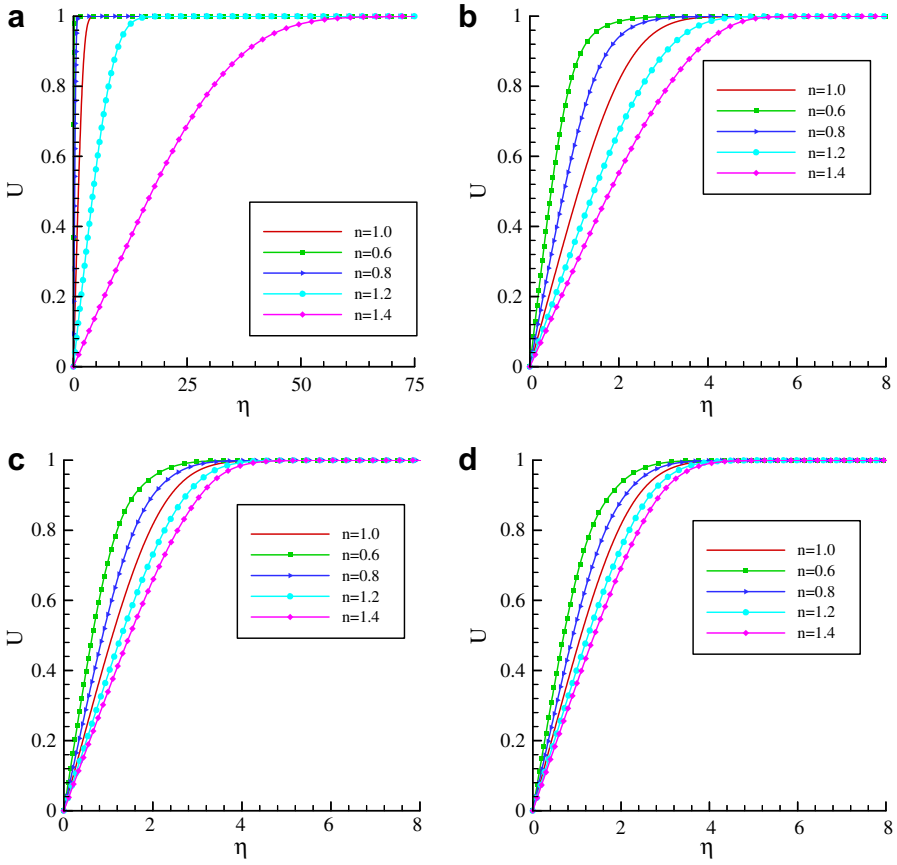

Fig. 3. Velocity distribution at (a) $\xi=0.0$ (b) $\xi=0.1075$ (c) $\xi=1.0102$ and (d) $\xi=2.0139$.

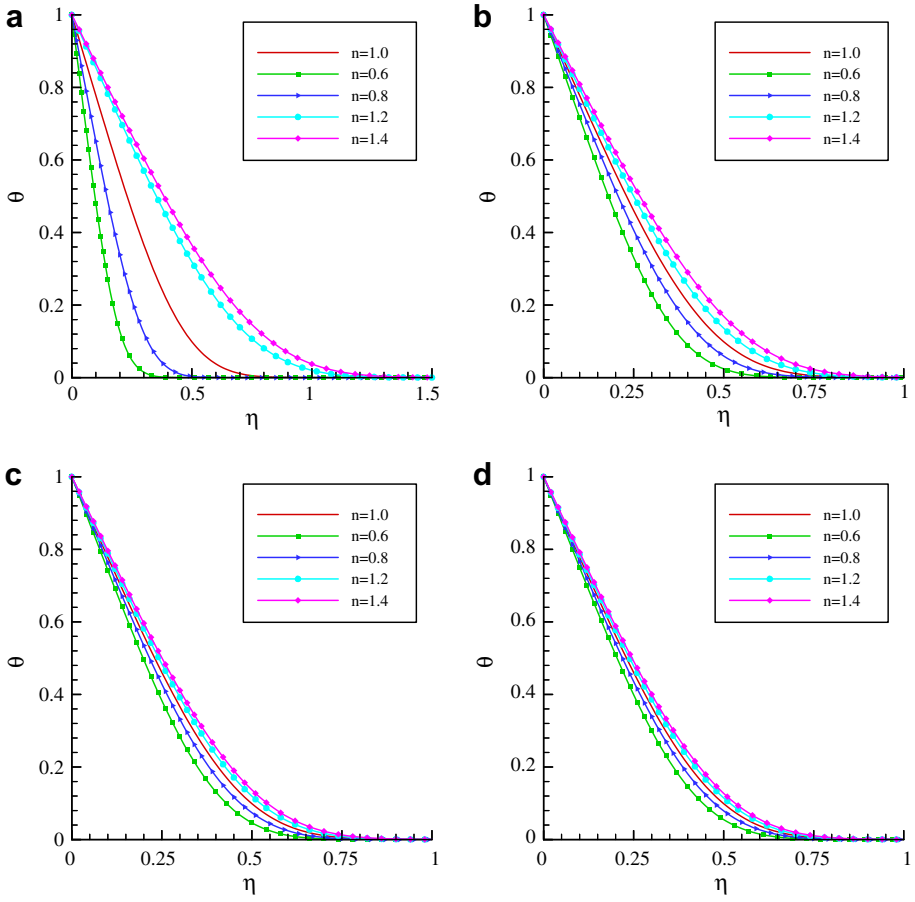

Fig. 4. Temperature distribution at (a) $\xi = 0.0$ (b) $\xi = 0.1075$ (c) $\xi = 1.0102$ and (d) $\xi = 2.0139$ while $Pr = 100$.

larger n, the thickness of the boundary layer is thinner. On the other hand, for the shear-thickening fluids ($n > 1$) the velocity decelerated slowly due to the large viscous effect, and the boundary layer is thicker near the leading edge. From Fig. 3b–d, we can say that, at the downstream region the velocity distribution gradually approaches the velocity distribution of the Newtonian fluid ($n = 1$). This means, for the shear thinning case, the effect of the viscosity increases while, for the shear-thickening case, it decreases in the downstream region. The distribution of shear stresses gradually smooths out, and so do the viscosities.

It is worthwhile to note that the boundary-layer thickness for $n = 1.4$ at $\xi = 0$ is approximate 75, but quickly drops below 10 before $\xi = 0.1$. This is because $n = 1.4$ is an extreme case, and the viscosity at $\xi = 0$ is about 15 times larger than that for $n = 1.2$. As soon as the fluid flows past the leading edge, the viscosity quickly drops, the local Reynolds number increases, and the boundary layer becomes thinner.

It is clear that the variation of boundary-layer thickness is large for non-Newtonian fluids. In particular, the Reynolds number at the leading edge for a shear-thickening fluid can be small; implying the boundary-layer approximation may be inappropriate. To apply the analysis reported in this paper requires a judgment to make sure that the boundary-layer approximation is appropriate. If the flow Reynolds number near the leading edge region is small; the axial diffusion terms become as large as the axial convection terms. Consequently, they cannot be ignored and no boundary-layer structure exists near the leading edge. However, the flow accelerates in the downstream direction, increasing the Reynolds number so that it becomes large enough to support a boundary layer. This is a complex problem, and has, to our knowledge, never been studied before. We will try to explain the complex nature of the problem below.

The flow physics of a boundary layer of a Newtonian fluid near a sharp leading edge is much simpler than the problem discussed above. Unfortunately, even this simpler case is still an open problem without a completely satisfactory solution. The leading-edge problem for a further simplified case of a slug flow has an analytical solution [17], which can reveal some of the proper physics near the leading edge and also provide an explanation of the singularity at the leading edge. Axial diffusion terms are as important as axial convection terms in a small leading-edge region whose size is of $O(Re^{-1})$. In this region the governing partial differential equation is elliptic and is not parabolic. The heating effect starts a short distance $O(\mathrm{Re}^{-1})$ ahead of the leading edge. This can be seen from many Schlieren pictures of boundary layers near a sharp leading edge. The analysis indicates that the thickness of boundary layers at the leading edge is $O(Re^{-1})$. This tiny thickness at the leading edge complicates analyses of boundary layers substantially. Since its size is $O(Re^{-1})$ and much smaller than the thickness of boundary layer, which is $O(Re^{-1/2})$, it is always assumed that the thickness of boundary layers is zero at a sharp leading edge. This is the source of the singularity associated with the leading edge of a sharp object. Fortunately, the strength of the singularity is $O(x^{-1/2})$, and hence integrable; thus, it can be scaled out, as demonstrated above. The acceptance of this simplification has been repeatedly verified experimentally, and has been taken for granted since the beginning of the boundary-layer theory. It should be noted that the size of the small Reynolds-number region for extreme shear-thickening, non-Newtonian fluids is not similar to the leading-edge region discussed above, and is currently unknown.

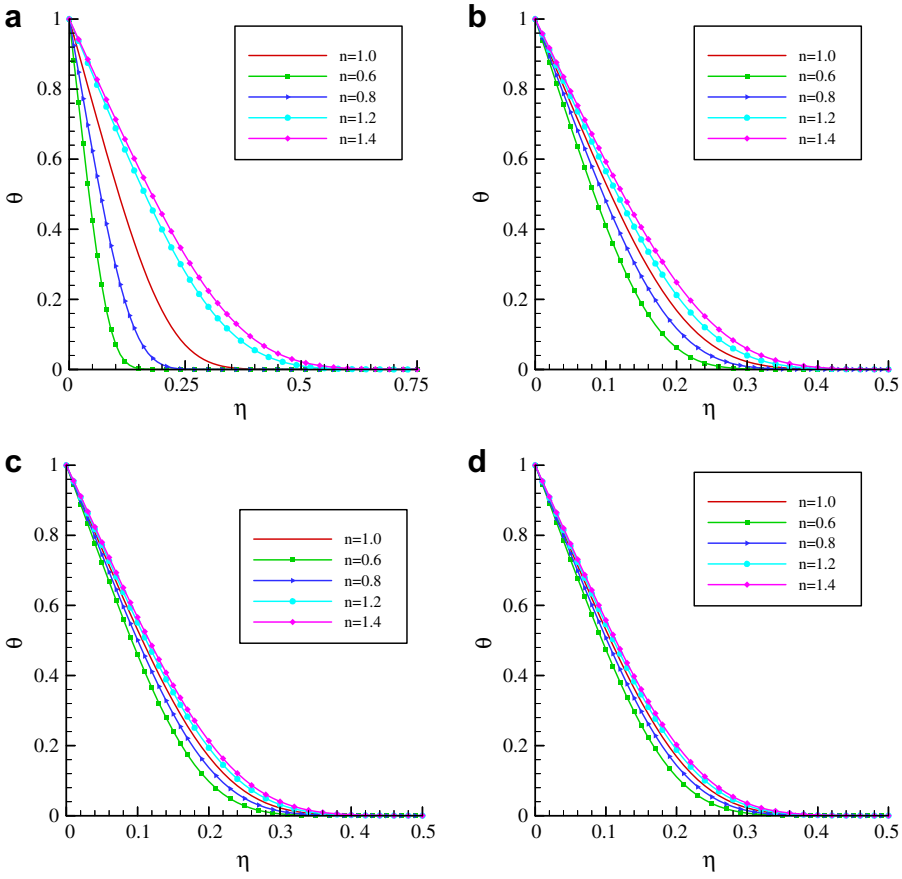

Fig. 5. Temperature distribution at (a) $\xi = 0.0$ (b) $\xi = 0.1075$ (c) $\xi = 1.0102$ and (d) $\xi = 2.0139$ while $Pr = 1000$.

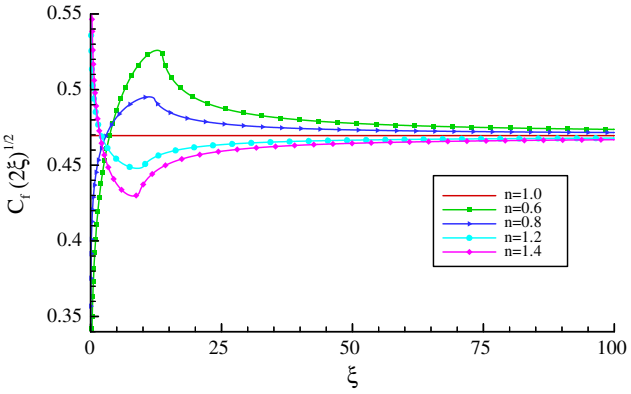

Fig. 6. Distribution of Nusselt number for $Pr = 100$.

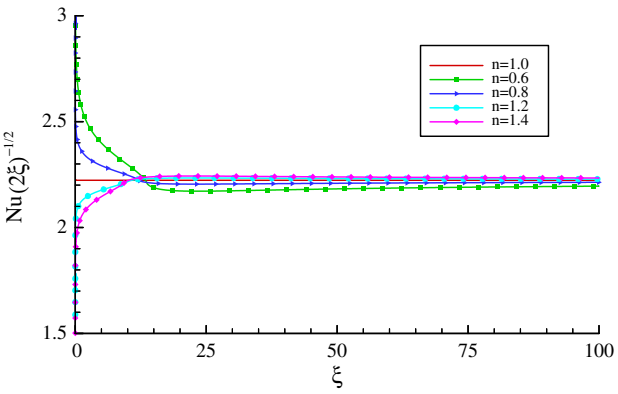

Fig. 7. Distribution of Nusselt number for $Pr = 1000$.

The corresponding temperature distribution are plotted for $Pr = 100$ and 1000 in Figs. 4 and 5, respectively. For both of these Prandtl numbers, in the case of shear thinning fluids, the temperature distributions are smaller than the distribution for the shear-thickening fluids. At the downstream region the temperature distribution increases for $n < 1$ and decreases for $n > 1$ case owing to the opposite viscous effect for the shear thinning and shear thickening fluids. Here it is notable that for $Pr = 1000$ the thermal boundary layer thickness is approximately half of that for $Pr = 100$. The variation of boundary-layer thickness, which is inversely proportional to the square root of the local Reynolds number, is clearly demonstrated in the plots of velocity and temperature distributions above.

The result of the variation of the wall shear stress is expressed in terms of the skin-friction coefficient $C_f(2\xi)^{1/2}$ in Fig. 6. The minimum wall shear stress of the shear-thinning fluids ($n < 1$) and the maximum wall shear stress of the shear-thickening fluids ($n > 1$) occur at the leading edge of the plate. For the shear-thinning case, the wall shear stress increases up to $\xi \approx 12.5$ and then gradually decreases and asymptotically approaches the value for a Newtonian fluid ($n = 1$). Similarly, for a shear-thickening fluid, the wall shear stress decreases up to $\xi \approx 10$ and then asymptotically approaches the wall shear of Newtonian fluid. In a computation up to $\xi = 8000$, the difference of the wall shear stress of non-Newtonian fluid and Newtonian fluids become extremely small, but still not identical. This is a result of the inherent non-linearity associated with the non-Newtonian fluid.

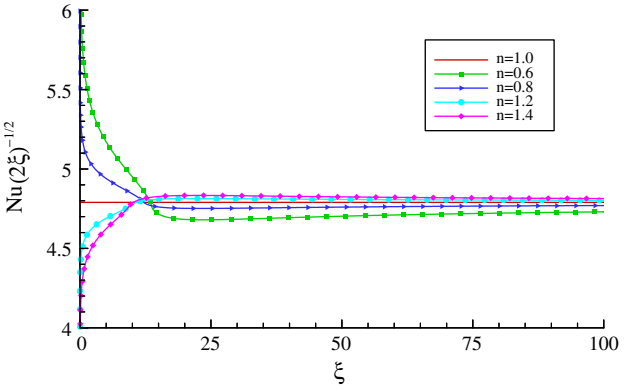

Fig. 8. Distribution of Nusselt number for $Pr = 1000$.

The rate of heat transfer in terms of the Nusselt number $Nu(2\xi)^{-1/2}$ are shown in Figs. 7 and 8, respectively for $Pr = 1000$ and 1000. For both Prandtl numbers, the maximum heat transfer rate occurs at the leading edge for non-Newtonian shear-thinning fluids. Specifically, for $n = 0.6$, the maximum values of $Nu(2\xi)^{-1/2}$ are 5.34706 and 11.9674 for $Pr = 1000$ and 1000, respectively. The minimum values of the heat transfer rate occur at the leading edge for the shear-thickening fluids; for $n = 1.4$, they are 1.33526 and 2.87654 with the respective Prandtl number 100 and 1000. After the leading edge, for $n < 1$ the rate of heat transfer decreases and for $n > 1$ increases suddenly up to $\xi \approx 12.5$ and then asymptotically approach the value of $Nu(2\xi)^{-1/2}$ in the case of Newtonian fluid. From Figs. 6–8, we can conclude that if the wall shear stress is large, the heat transfer rate is small, and vice versa.

4. Conclusions

The proposed modified power-law correlation fits well with the measurement of non-Newtonian fluids; consequently it does not contain physically unrealistic limits. The problems associated with the non-removal singularity introduced by the traditional power-law correlations are eliminated by use of the modified power-law correlation proposed in this paper. Therefore, it can be used to investigate other heat transfer problems for shear thinning or shear thickening, non-Newtonian fluids in boundary layers.

References

[1] J. Hinch, Non-Newtonian geophysical fluid dynamics, 2003 Program in Geophysical Fluid Dynamics, Woods Hole Oceanographic Institution Woods Hole, MA 02543 USA. http://gfd.whoi.edu/proceedings/2003/PDFvol2003.html.
[2] A. Acrivos, A theoretical analysis of laminar natural convection heat transfer to non-Newtonian fluids, AIChE J. 16 (1960) 584–590.
[3] F. Emery, H.S. Chi, J.D. Dale, Free convection through vertical plane layers of non-Newtonian power-law fluids, ASME J. Heat Transfer 93 (1970) 164–171.
[4] T.V.W. Chen, D.E. Wollersheim, Free convection at a vertical plate with uniform flux conditions in non-Newtonian power-law fluids, ASME J. Heat Transfer 95 (1973) 123–124.
[5] Z.P. Shulman, V.I. Baikov, E.A. Zaltsgendler, An approach to prediction of free convection in non-Newtonian fluids, Int. J. Heat Mass Transfer 19 (1976) 1003–1007.
[6] A. Som, J.L.S. Chen, Free convection of non-Newtonian fluids over non-isothermal two-dimensional bodies, Int. J. Heat Mass Transfer 27 (1984) 791–794.
[7] S. Haq, C. Kleinstreuer, J.C. Mulligan, Transient free convection of a non-Newtonian fluid along a vertical wall, ASME J. Heat Transfer 110 (1988) 604–607.
[8] M.J. Huang, J.S. Huang, Y.L. Chou, C.K. Cheng, Effects of Prandtl number on free convection heat transfer from a vertical plate to a non-Newtonian fluid, ASME J. Heat Transfer 111 (1989) 189–191.
[9] M.J. Huang, C.K. Chen, Local similarity solutions of free-convective heat transfer from a vertical plate to non-Newtonian power-law fluids, Int. J. Heat Mass Transfer 33 (1990) 119–125.
[10] E. Kim, Natural convection along a wavy vertical plate to non-Newtonian fluids, Int. J. Heat Mass Transfer 40 (1997) 3069–3078.
[11] W.A. Khan, J.R. Culham, M.M. Yovanovich, Fluid flow and heat transfer in power-law fluids across circular cylinders: analytical study, J. Heat Transfer 128 (2006) 870–878.
[12] J.P. Denier, P.P. Dabrowski, Asymptotic matching constraints for a boundary-layer flow of a power-law fluid, J. Fluid Mech. 460 (2004) 261–279.
[13] J.P. Denier, R.E. Hewitt, Laminar natural convection heat transfer to non-Newtonian fluids, Appl. Sci. Res. 17 (2004) 233–248.
[14] L.S. Yao, M.M. Molla, Flow of non-Newtonian fluids on a flat plate: I. boundary layer, J. Thermophys. Heat Transfer, in press.
[15] M.M. Molla, L.S. Yao, Flow of non-Newtonian fluids on a flat plate: II. Heat transfer, J. Thermophys. Heat Transfer, in press.
[16] L.S. Yao, Two-dimensional mixed convection along a flat plate, ASME J. Heat Transfer 109 (1987) 440–445.
[17] L.S. Yao, C.L. Tien, S.A. Berger, Thermal analysis of a fast moving slab between two adjacent temperature chambers, J. Heat Transfer 98 (1976) 326–329.